

PACS numbers: 61.72.Uj, 78.20.Ci, 78.30.FS, 78.55.Et

**TEMPERATURE INDUCED STRESS DEPENDENT  
PHOTOLUMINESCENCE PROPERTIES OF NANOCRYSTALLITE ZINC  
OXIDE**

**V. Kumar<sup>1</sup>, R.G. Singh<sup>2</sup>, L.P. Purohit<sup>1</sup>, R.M. Mehra<sup>3</sup>**

<sup>1</sup> Department of Physics,  
Gurukul Kangri University, Haridwar – 249 404, India  
E-mail: [vinod.phy@gmail.com](mailto:vinod.phy@gmail.com)

<sup>2</sup> Department of Electronic Science,  
University of Delhi South Campus, New Delhi – 110 021, India

<sup>3</sup> School of Engineering & Technology, Sharda University,  
Greater Noida – 201306, India

*In this paper, Temperature induced stress dependent structural, optical and photoluminescence properties of nanocrystallites ZnO (nc-ZnO) films are reported. It is seen that crystallite size, band gap and PL intensity of nc-ZnO are strongly dependent on stress. Large compressive stress has been observed at temperature 350-400 °C while minimum stress obtained at temperature 450 °C. A small amount of expensive stress is obtained at temperature 500 and 500 °C. The surface topography of the nc-ZnO films has been studied using atomic force microscopy. The optical band gap of nc-ZnO has been decreased from 3.25 to 3.23 eV as a function of temperature induced stress. The luminescence property is dependent on stress of nc-ZnO films.*

**Keywords:** SOL-GEL, STRESS, TOPOGRAPHY, PHOTOLUMINESCENCE, BAND GAP NARROWING.

*(Received 04 February 2011, in final form 02 May 2011)*

## 1. INTRODUCTION

The metal oxide semiconductor ZnO has gained substantial interest in the research community in past decade because of its large exciton binding energy (60 meV) and efficient radiative recombination [1]. The large exciton binding energy paves the way for an intense near band – edge excitonic emission at room and even higher temperatures which leads to lasing action based on exciton recombination and possibly polariton / exciton interaction even above room temperature. ZnO has a hexagonal wurtzite (Wz) structure where each anion is surrounded by four cations at the corners of a tetrahedron and vice versa. ZnO is an alternative material to indium tin oxide (ITO) which has been mostly used now a day for many optoelectronics applications [2]. ZnO is a technologically important material exhibiting multifunctional properties for various applications in optoelectronic devices, such as solar cell transparent conducting electrodes, heat mirrors [3-5], Light emitting diodes and light extraction enhancement devices [6].

Intrinsic and extrinsic stress are inevitably found in ZnO. The intrinsic stress is associated with defect and impurities. The extrinsic stress is mainly related to the lattice mismatch, thermal mismatch, doping and growth

condition. Stress in film provides useful information about defect evolutions which is very important for better understanding and improving the electrical and optical properties [7]. On the other hand, it is realized that the band gap of ZnO may change with the stress and will subsequently modify the optical and electrical characteristics. Therefore, the stress induced effects are becoming critical to the fabrication of ZnO-based devices. However, there are very few studies concerning the stress in ZnO films by far and our knowledge in this regard remains insufficient.

In the present work, we have studied temperature induced stress dependent structural, optical and photoluminescence properties of nc-ZnO films grown by sol-gel method using spin coating technique. A strong dependence of crystallite size, photoluminescence and band gap and on the stress has been investigated. Annealing dependent surface morphology is also investigated.

## 2. EXPERIMENTAL

Zinc Oxide thin films were deposited on glass substrate by spin coating technique. Zinc acetate dihydrate [ $\text{Zn}(\text{CH}_3\text{COO})_2 \cdot 2\text{H}_2\text{O}$ ] (purity 99.95 %) (Merck Extra pure chemical Ind. Ltd, India) was used as a source of zinc. Ethanol (AR, Merck chemicals, India) and Monoethanolamine [MEA] (Merck, India) were used as the solvent and stabilizer respectively. The Zn precursor solution was prepared by dissolving zinc acetate dihydrate in ethanol so as prepare concentration of 0.2 mol/l. MEA was then added in the solution. The molar ratio MEA/Zn was fixed to 1. The mixture was stirred ultrasonically at 25 °C for 2 hours. The clear transparent and homogenous solution thus obtained was left for ageing for 72 hours. Substrates were ultrasonically cleaned using acetone, methanol and deionized water sequentially for 15 min each. One drop of solution was dropped onto the substrate which was rotated at 2500 rpm for 30 sec by a spin coater. After deposition by spin coating, the films were dried in air for 10 min over hot plate to evaporate the solvent and remove organic residuals. The process from coating to drying has been repeated for fifteen times to be obtained the desired films thickness. The films were then annealed in air at temperature range 350-550°C for 1 hour in a microprocessor controlled furnace by a heating rate 5°/min.

Crystalline nature of the ZnO films was confirmed by PAN alytical X'pert PRO diffractometer using the  $\text{CuK}_\alpha$  radiation having a wavelength 1.5140 Å. The film thickness was measured by surface profiler ambious XP-1. The topography of the nc-ZnO films was analysed by a Digital Nanoscope III a SPM. Photoluminescence (PL) measurements were performed on a Perkin – Elmer LS 55 spectrophotometer. The band gap of ZnO films were measured by optical transmittance using a Shimadzu Solid Spec 3700 double beam spectrophotometer.

## 3. RESULTS AND DISCUSSION

### 3.1 Structural analysis

XRD was used to analyze the growth orientation and determine the crystallite size of nc-ZnO. The effect of annealing temperature on XRD pattern of nc-ZnO is shown in Fig. 1 a. All the films exhibit preferential orientation c – axis (002) peak perpendicular to the substrate surface having

wurtzite structure as reported in literature JCPDS card no 79 – 0206. Fig. 1b shows the effect of annealing temperature on the integrated intensity of XRD data. Maximum intensity is obtained at annealing temperature 450 °C due to the minimum stress in films. The crystallite size of nc-ZnO can be calculated from the integral width of the (002) line according to Scherrer's formula [8],

$$D = \frac{k\lambda}{\beta \cos \theta} \quad (1)$$

Where  $D$  is the diameter of the crystallites forming into the films,  $\lambda$  is the wavelength of  $\text{CuK}_\alpha$  radiation (0.15406 Å),  $k$  is correlation factor (0.94),  $\beta$  is full width half maxima (FWHM) of (002) peak and  $\theta$  is Bragg diffraction angle. Fig. 1c shows the effect of annealing temperature on crystallite size. Crystallite size is increasing continuously with increase annealing temperature. It is observed that the peak position angle shifts towards the higher  $\theta$  value.

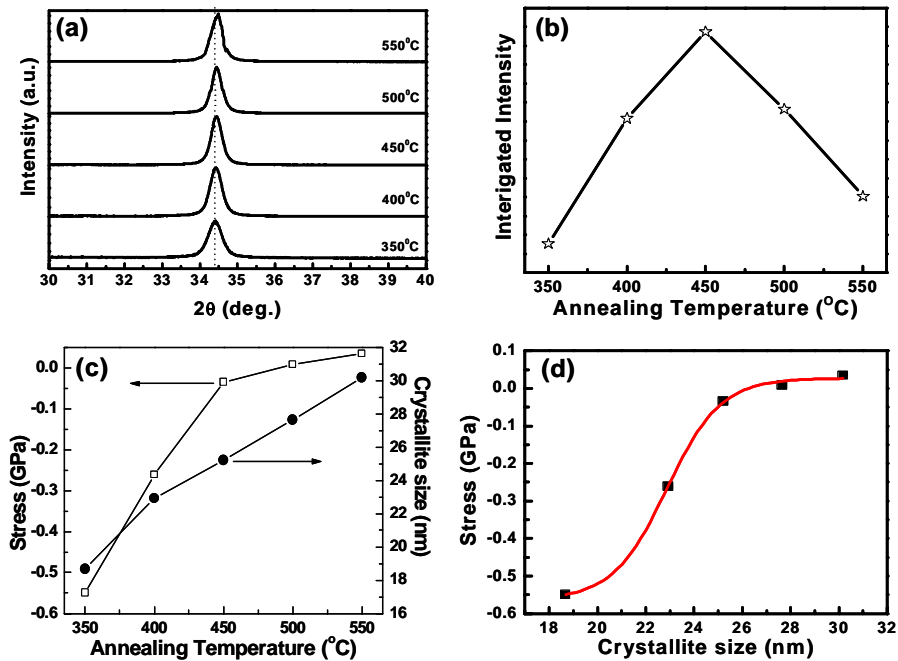


**Fig. 1** – XRD pattern of ZnO films as a function of annealing temperature (a), Effect of annealing temperature on the integrated intensity of XRD in ZnO (b), Variation of crystallite size and stress with different annealing temperature, (c), and graph between crystallite size versus stress of the film (d)

The (002) peak position is indicating change in the direction of stress compared to unstressed film. The stress in the film can be calculated by the biaxial strain model [9]

$$\sigma = \frac{2c_{13}^2 - c_{33}(c_{11} + c_{12})}{c_{13}} \left( \frac{c - c_0}{c_0} \right) \quad (2)$$

Where,  $c_{11} = 209.7$  GPa,  $c_{12} = 121.1$  GPa,  $c_{13} = 105.1$  GPa,  $c_{33} = 210.9$  GPa are the elastic stiffness constants of bulk ZnO.  $c_0$  (0.52055 nm) is the stress free lattice constant. Annealing temperature dependent stress in nc-ZnO films is shown in Fig. 1 c. The value of stress is varying from  $-0.549$  to  $0.0348$  GPa with change in annealing temperature from  $350$  to  $550$  °C. nc-ZnO has shown a compressive stress at lower annealing temperature and minimum stress is obtained at annealing temperature  $450$  °C. The stress in nc-ZnO is caused by the structural defect and growth conditions (environment, annealing temperature). We have shown the correlation between the crystallite size and stress of nc-ZnO in Fig. 1 d. The crystallite size of nc-ZnO has been increased with increase annealing temperature attributed to the lattice mismatching and thermal mismatching of the film and substrate. Maximum crystallite size of nc-ZnO has been obtained at minimum stress. This is indicating that the stress is directly correlated to the crystallite size of nc-ZnO. We propose a relation between stress and crystallite size by stimulating the experimental data using mathematical tool.

$$\sigma = 0.02733 - 0.58983 \left\{ 1 + \exp \left( \frac{D - 22.876}{1.115} \right) \right\} \quad (3)$$

From the above relationship, we can say that the stress of nc-ZnO along c-axis is sigmoidally (sigmoidal fitting) related to crystallite size or vice-versa. Fig. 1 d shows the presence of compressive stress when crystallite size is small (19-23 nm). A stress free and expansive stress film is obtained at large crystallite size (25-30 nm).

### 3.2 Surface morphology

The surface topography of the annealed films was studied using atomic force microscopy (AFM) in the tapping mode. Figure 2 shows the AFM images of nc-ZnO films scanned over an area of  $1.0 \mu\text{m}^2$  annealed at  $350$ ,  $450$  and  $500$  °C. It shows the hexagonally faceted columnar grains that dominates the surface morphology. It can be observed that with increase in annealing temperature, the surface roughness of the film decreases dramatically (from  $10.534$  nm to  $8.43$  nm) up to  $450$  °C. The change in crystallinity and morphology is attributed to the stress of films.

Li et al. [10] reported that surface morphology could be attributed to a thermally induced stress film. The increase of annealing temperature shows a process of coalescence resulting in the occurrence of grain growth. At high temperature, the atoms have enough diffusion/activation energy to occupy the correct site in the crystal lattice and grains with the lower surface energy will become larger at high temperature.

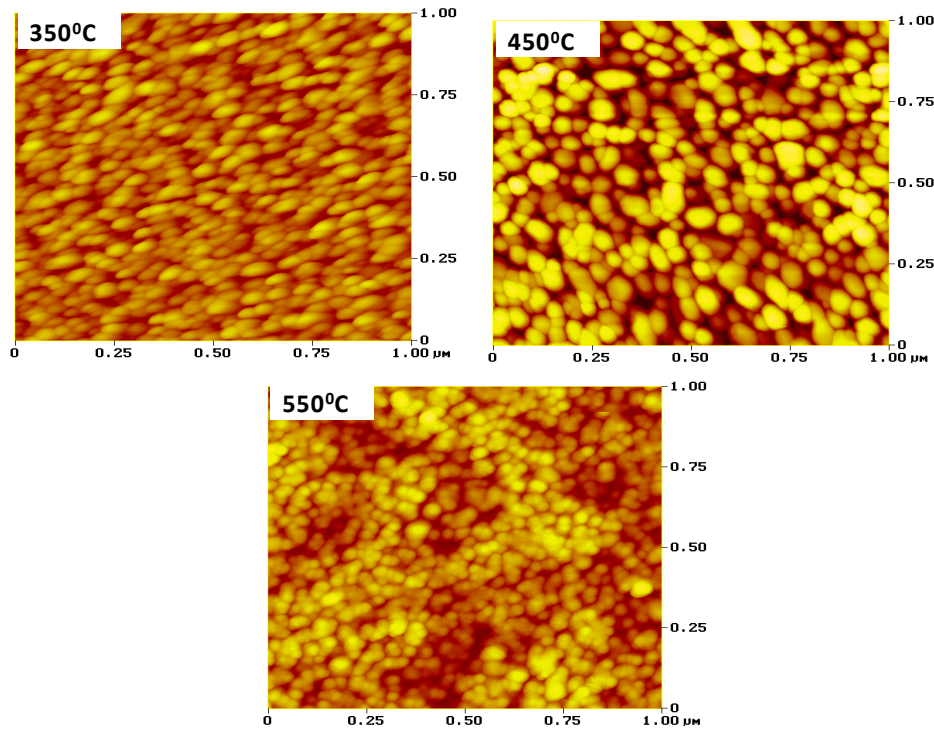


*Fig. 2 – AFM images of nc-ZnO at different annealing temperature*

### 3.3 Photoluminescence properties of nc-ZnO

Photoluminescence spectra of nc-ZnO films in the range 300 to 750 nm are shown in Fig. 3 a. Various mechanisms have been proposed to understand the visible luminescence in ZnO. Vanheusden et al. has found that singly ionized oxygen vacancies ( $V^*$ ) are responsible for the green luminescence in the ZnO [11]. Oxygen vacancies occur in three charge states: the neutral oxygen vacancy ( $Vo^*$ ), singly ionized oxygen vacancy ( $Vo$ ), and doubly ionized oxygen vacancy ( $Vo^{**}$ ). The singly ionized oxygen vacancy ( $Vo^*$ ) gives the emission, so called luminescence centers [12]. The excitation luminescence may be due to increased defect concentration through trapping or non-radioactive recombination [13]. All the films are showing only the blue emission peak at peak position (423 nm), which is associated with deep level defects in ZnO. We have tried to understand of the observed PL emission in terms of stress induced defect usually attributed to structural defect, which in turn is due to zinc vacancy (VZn), oxygen vacancy (Vo), zinc interstitial (Zni), and oxygen interstitial (Oi). The visible luminescence (400-525 nm) of nc-ZnO increases with increase in annealing temperature. Peak position of PL spectra is shifted to higher wavelength region (red shift).

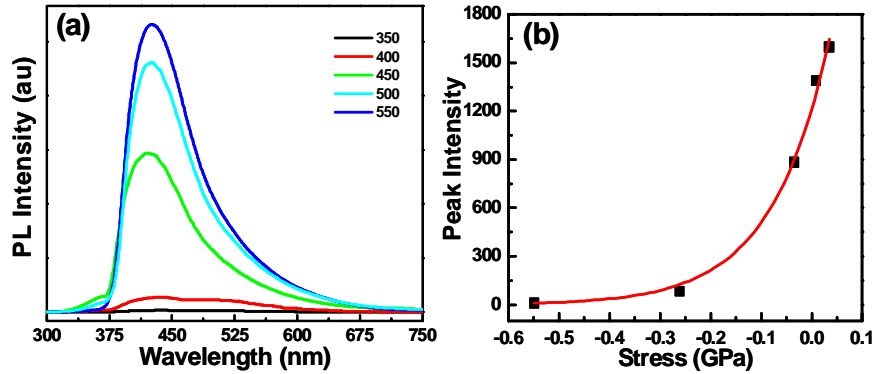


**Fig. 3** – Photoluminescence (PL) spectra of ZnO films annealed at different temperature (a), Plot of peak Intensity versus stress along c-axis of ZnO films (b). The solid line represents an exponential fitting result to the experimental data; value of fitting parameter has been disuses in text of figure

Fig. 3 b shows the relation between PL intensity and stress. Intensity of PL spectra is increased with increase in annealing temperature attributed to the stress of nc-ZnO films. Compressive stress is providing a luminescence killer and expensive stress provided luminescence centre. We have proposed a relation between PL intensity and stress of nc-ZnO films,

$$PI = 1215.6 \exp\left(\frac{-\sigma}{0.11513}\right) \quad (4)$$

The experimental data has been fitted to an approximate exponential growth dependence on the peak intensity with stress. Above equation has been found that the integrated intensity is strongly dependent on stress.

### 3.4 Band gap narrowing of nc-ZnO

Fig. 4(a) represents the optical transmittance spectra of nc-ZnO at different annealing temperatures in the range 300 to 1000 nm. The average transmission within the visible region for all the films was higher than 85 %. It is clearly seen from the figure that the UV absorption edge is shifted towards red with increase in annealing temperature. This is indicating the narrowing of the optical band gap. For the allowed direct transition, the variation of  $\alpha$  with photon energy ( $h\nu$ ) obey Tauc's plot method [14],

$$(\alpha h\nu)^2 = A(h\nu - E_g) \quad (5)$$

Where,  $A$  is a constant,  $E_g$  is optical band gap,  $h$  is plank constant and  $\alpha$  is the absorption coefficient. A plot of  $(\alpha h\nu)^2$  versus  $h\nu$  often yield a reasonably good straight line fit of the absorption edge for the films. The point on extrapolation of  $h\nu$  at which  $\alpha^2 = 0$  provides a convenient experimental benchmark to find optical band gap.

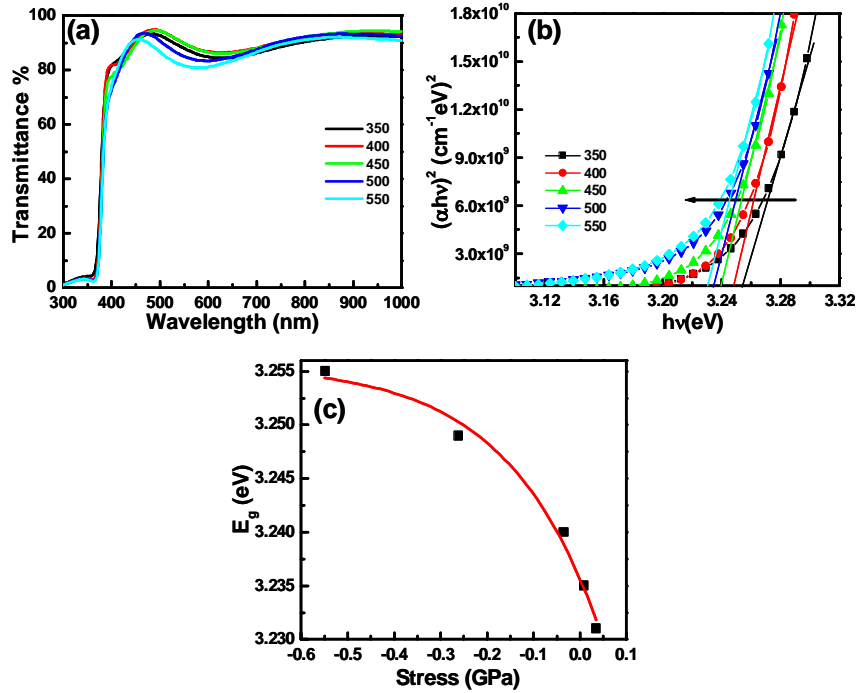


**Fig. 4** – Optical Transmittance spectra of ZnO films at different annealing temperature (a), Band gap variation of ZnO films with annealing temperature, calculated by Tauc's plot method and a arrow shows the band gap narrowing behavior (b). To understand the band gap narrowing, a graph plot between band gap and stress and Boltzmann fitting and fitting value has been discuss with in text (c)

The plot of  $(\alpha h\nu)^2$  versus photon energy  $h\nu$  for nc-ZnO annealed at different temperatures is shown in Fig. 4b. The band gap of nc-ZnO decreases from 3.26 to 3.23 eV with increase in annealing temperature from 350 to 550 °C. The effect of stress on the band gap of nc-ZnO is shown in Fig. 4 c. A sigmoidal relation between band gap and stress has been developed here,

$$E_g = 2.4517 + 0.8039 \left\{ 1 + \exp \left( \frac{\sigma - 0.713}{0.194} \right) \right\} \quad (6)$$

Band gap of nc-ZnO films is decreasing with change in stress from compressive to expansive. The compressed lattice is expected to provide a wide band gap because of the increase repulsion between the oxygen 2 *p* and the zinc 4s bands [15].

#### 4. CONCLUSIONS

High quality nc-ZnO films have been prepared by sol-gel method using spin coating technique. Our results showed that the temperature induced photoluminescence and optical properties are directly correlated to the stress of films. Band gap of nc-ZnO is decrease with transition of stress from compressive to expensive. Minimum stress has been obtained at annealing

temperature 450 °C. PL intensity is increased with the transition of stress from compressive to expansive. These nc-ZnO films give the new opportunities for optoelectronic device.

#### 4. ACKNOWLEDGMENT

The authors are wish to thanks Dr. D. K. Avasthi, IUAC New Delhi for AFM measurement.

#### REFERENCES

1. W.Y. Liang, A.D. Yoffe, *Phys. Rev. Lett.* **20**, 59 (1968).
2. V. Shelke, B.K. Sonawane, M.P. Bhole, D.S. Patil, *J. Non-Cryst. Solids* **355**, 840 (2009).
3. J.A. Aranovich, D. Golmayo, A.L. Fahrenbruch, R.H. Bube, *J. Appl. Phys.* **51**, 4260 (1980).
4. V. Srikant, D.R. Clarke, *J. Appl. Phys.* **81**, 6357 (1997).
5. T. Minami, H. Nanto, S.A. Takata, *Thin Solid Films* **124**, 43 (1985).
6. M.D. McCluskey, S.J. Jokela, *J. Appl. Phys.* **106**, 071101 (2009).
7. B.C. Mohanty, Y.H. Jo, D.H. Yeon, I.J. Choi, Y.S. Cho, *Appl. Phys. Lett.* **95**, 062103 (2009).
8. Y. Natsume, H. Sakata, *Mater. Chem. Phys* **78**, 170 (2002).
9. M.K. Puchert, P.Y. Timbrell, R.N. Lamb, *J. Vac. Sci. Tech. A* **14**, 2220 (1996).
10. Y.F. Li, B. Yao, Y.M. Lu, C.X. Cong, Z.Z. Zhang, Y.Q. Gai, C.J. Zheng, B.H. Li, Z.P. Wei, D.Z. Shen, X.W. Fan, L. Xiao, S.C. Xu, Y. Liu, *Appl. Phys. Lett.* **91**, 021915 (2007).
11. K. Vanheusden, W.L. Warren, C.H. Seager, D.R. Tallant, J.A. Voigt, B.E. Gnade, *J. Appl. Phys.* **79**, 7983 (1996).
12. L.V. Azaroff, *Introduction to Solid* (Mc Graw Hill, pp. 371-372, 1960).
13. A.B. Djurisic, Y.H. Leung, K.H. Tam, Y.F. Hsu, L. Ding, W.K. Ge, Y.C. Zhong, K.S. Wong, W.K. Chan, H.L. Tam, K.W. Cheah, W.M. Kwok, D.L. Philips, *Nanotechnology* **18**, 095702 (2007).
14. J. Tauc, R. Grigorovici, A. Vancu, *phys. status solidi B* **15**, 627 (1966).
15. R. Gosh, D. Bashk, S. Fujihara, *J. Appl. Phys.* **96**, 2689 (2004).